

Current transport along the [001] axis of YBCO in low-temperature superconductor—normal metal—high-temperature superconductor heterostructures

F. V. Komissinskiĭ

*Institute of Radio Engineering and Electronics, Russian Academy of Sciences, 103907 Moscow, Russia;
M. V. Lomonosov Moscow State University, 119899 Moscow, Russia*

G. A. Ovsyannikov^{*})

Institute of Radio Engineering and Electronics, Russian Academy of Sciences, 103907 Moscow, Russia

N. A. Tulina and V. V. Ryazanov

Institute of Solid-State Physics, Russian Academy of Sciences, 142432 Chernogolovka, Moscow Region, Russia

(Submitted 27 May 1998; resubmitted 14 July 1999)

Zh. Éksp. Teor. Fiz. **116**, 2140–2149 (December 1999)

The electrophysical properties of heterojunctions several microns in size, obtained by successive deposition of the metal-oxide high-temperature superconductor $\text{YBa}_2\text{Cu}_3\text{O}_x$, a normal metal Au, and the low-temperature superconductor Nb, were studied experimentally. Current flows in the [001] direction of the epitaxial $\text{YBa}_2\text{Cu}_3\text{O}_x$ film. It is shown, by comparing the experimental data with existing theoretical calculations, that for the experimentally realizable transmittances ($\bar{D} = 10^{-5} - 10^{-6}$) of the $\text{YBa}_2\text{Cu}_3\text{O}_x$ —normal metal boundary the critical current of the entire heterostructure is low (of the order of the fluctuation current) because of a sharp change in the amplitude of the potential of the superconducting carriers at this boundary. The current–voltage characteristics of the heterostructure studied correspond to tunnel junctions consisting of a superconductor with $d_{x^2-y^2}$ type symmetry of the superconducting wave function and a normal metal. © 1999 American Institute of Physics. [S1063-7761(99)02012-0]

1. INTRODUCTION

Currently many properties of HTSCs are being estimated using a d -type wave function for the superconducting carriers. Specifically, this model explains the magnetic field dependence of the critical current in bimetallic two-junction SQUIDS consisting of $\text{YBa}_2\text{Cu}_3\text{O}_x$ (YBCO) and Pd¹ and the spontaneous excitation of magnetic flux quanta in HTSC structures with three bicrystalline boundaries.² At the same time, experiments on electron tunneling in the c direction in HTSCs give contradictory results. On the one hand, in HTSC—low-temperature superconductor (s -type superconducting wave function) junctions there is no critical current for junctions in the c direction,^{3–5} which agrees well with the theory of junctions consisting of superconductors with a d -type wave function for the superconducting carriers and an s -superconductor. On the other hand, an appreciable critical current, whose amplitude varies nonmonotonically as a function of the magnetic and microwave fields nonmonotonically as predicted for junctions with s -superconductors, has been observed in a number of experiments.^{6–8} To explain the experiments of Refs. 6–8, it has been conjectured that in yttrium-group HTSC materials a mixture of superconducting s - and d -type carriers arises because of the orthorhombic nature of these materials, and diffuse scattering near the boundary or twinning of HTSC films results in a larger contribution from the s component.^{9,10} We note that an estimate of the parameters of the Pb/(Au,Ag)/YBCO structures inves-

tigated in Refs. 6–8 gives transmittances $D = 10^{-7} - 10^{-9}$, averaged over the directions of the moments, for the barriers of the HTSC—normal metal barriers with quite large junction areas, $S = 0.1 - 1 \text{ mm}^2$.

In the present paper we report the results of an experimental investigation of current flow in s -superconductor—normal metal—HTSC heterojunctions, fabricated by successive deposition of YBCO, a normal metal (ordinarily Au), and Nb, with much smaller areas ($S \approx 8 \times 8 \mu\text{m}^2$) and higher transmittance ($10^{-5} - 10^{-6}$) of the YBCO—normal metal boundary. The experimental data are analyzed from two standpoints: on the basis of the isotropic theory of s superconductivity and from the standpoint of the modern theory, which assumes a d -type wave function in the superconductor YBCO film.

2. EXPERIMENTAL PROCEDURE AND EXPERIMENTAL SAMPLES

The junctions were prepared by using the sequence of operations shown in Fig. 1. First, the epitaxial YBCO films were grown either by laser ablation or using cathodic sputtering in a diode configuration with dc current and high oxygen pressure. During YBCO film growth, a temperature 700–800 °C was maintained and the pure oxygen pressure was 0.3–1 mbar for laser ablation and 3 mbar for cathodic sputtering. Neodymium gallate with (110) orientation or the r plane of sapphire with a CeO_2 buffer layer was used as the

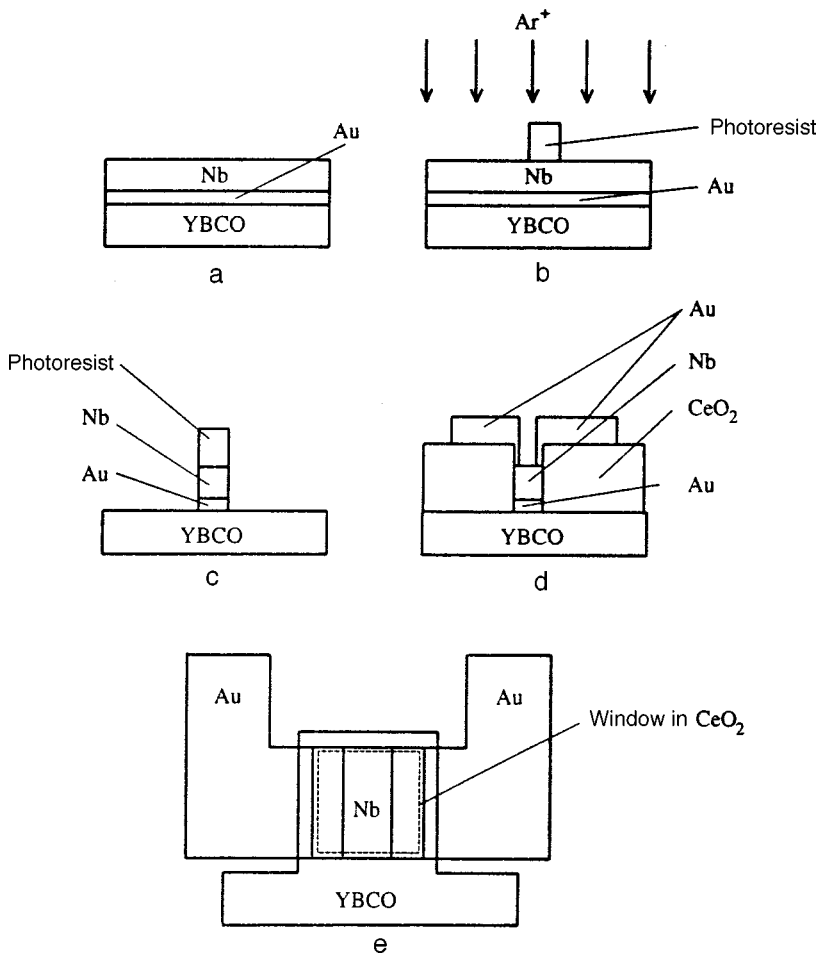


FIG. 1. Sequence for the preparation of HTSC–normal metal–superconductor heterostructures: a) deposition of a trilayer heterostructure Nb/Au/YBCO; b) formation of a region of the heterojunction using ionic etching; c) deposition of the insulator CeO₂ to prevent contacts with YBCO in the basal plane; d) fabrication of an Au electric layout; e) top view of the fabricated heterostructures.

substrate. Epitaxial YBCO films, 100–150 nm thick, with *c* orientation and the following superconducting parameters, measured by the resistive method, were obtained: 1) the critical temperature at which the resistance of the film deposited on a 5 × 5 mm² substrate is zero, $T_{cf} = 84 - 89$ K; 2) the width of the superconducting transition (determined at the levels 0.9 and 0.1 times the resistance of the film at the onset of the transition into the superconducting state), $\Delta T_c = 0.5 - 1$ K; 3) the ratio of the resistances at temperatures 300 K and 100 K, $\rho_{300\text{K}}/\rho_{100\text{K}} \approx 2.8$. The number of 0.3–1 μm in diameter particles on the surface of the YBCO film, which are caused by the formation of different phases of YBCO as well as Y, Ba, and Cu oxides, was $\sim 10^6\text{ cm}^{-2}$. Evidence of the high quality of the YBCO films fabricated is the small width of the (005) x-ray peak of YBCO, $\text{FWHM}(005) \approx 0.2^\circ$, for $\theta/2\theta$ scanning with 0.15 μm film thickness.

A thin, 20 nm thick, layer of normal metal (Au, Ag, Pt) was deposited at 100 °C immediately after the YBCO film, using either laser ablation or high-frequency cathodic sputtering (Fig. 1a). Next, a 100–150 nm thick Nb layer was deposited on a water-cooled substrate by a magnetron cathodic sputtering. The critical temperature of the superconducting transition in Nb films was 9.1–9.2 K. Niobium is used as the low-temperature superconductor because it does not enter into a solid-phase chemical reaction with Au. We note that in the experiments of Refs. 4–7, where Pb is used, a superconducting alloy of Au and Pb can form.

In the trilayer heterostructure obtained, photolithography and ion and plasma-chemical etchings were used to form regions of heterojunctions which during photolithography were fixed on sections with the minimum number of particles on the surface of the YBCO films (Fig. 1b). To prevent electrical contact in the basal (*a*–*b*) plane of the YBCO film, the lateral region of the junction was insulated with a CuO₂ layer with a central window with the dimensions $S = 8 \times 8\ \mu\text{m}^2$ (Fig. 1c). At the final stage explosion lithography was used to form junction areas and Au wiring in the form of two stripes, which enable separated input of current and voltage to the top electrode Nb (Figs. 1d, e). The geometry used for the gold contacts (see Fig. 1) makes it possible to investigate the electrophysical properties of Nb/Au/YBCO structures for the YBCO film in the superconducting state. More than 30 Nb/normal metal/YBCO samples, where Au, Ag, and Pt were used as the normal metal, were prepared. In the present paper the results of investigations performed on nine Nb/Au/YBCO samples, in which the variance of the characteristic resistances $R_N S$ (R_N is the differential resistance, measured for $V > 20$ mV) of the boundaries at liquid-helium temperature did not exceed a factor of 4 (see Table I).

3. EXPERIMENTAL RESULTS

The dependences of the resistances *R* of the heterojunctions on the temperature *T* and 4 μm wide the test bridges,

TABLE I. Electrophysical parameters of superconductor structures measured at $T=4.2$ K.

Sample	$R_d(0)$, Ω	R_N , Ω	$R_N S$, $10^{-6} \Omega \cdot \text{cm}^2$	$R_d(0)/R_N$	\bar{D} , 10^{-6}
P9J2	12.2	7.0	4.5	1.7	4.8
P9J3	9.8	6.0	3.8	1.6	5.6
P10J2	10.5	5.9	3.8	1.8	5.6
P10J3	10.6	5.9	3.8	1.80	5.6
P11J2	4.9	4.2	2.7	1.2	7.9
P11J3	5.2	3.6	2.3	1.4	9.3
P12J2	2.4	2.0	1.3	1.2	16.7
P13J2	7.2	3.5	2.2	2.1	9.5
P13J3	7.5	6.6	4.2	1.1	5.1

consisting of YBCO films placed on the same substrate, with 1–5 μA bias currents and their current-voltage characteristics (IVCs) in the temperature 4.2–300 K were measured. Figure 2 shows the temperature dependences for one of the substrates. At temperatures $T > T_{cf}$ metallic behavior of $R(T)$ is observed, i.e., the resistance decreases with temperature, as is characteristic for a c -oriented YBCO film with current flow in the basal plane of YBCO. As a rule, T_{cf} of the bridges and heterojunctions was less than the critical temperature of YBCO films, measured immediately after the trilayer heterostructure was prepared. The degradation of the superconducting properties of the film is evidently due to a decrease in the amount of oxygen during ionic etching. The inset in Fig. 2 shows the function $R(T)$ for a heterojunction at temperatures $T < T_{cf}$, demonstrating that the resistance of the heterojunction increases as temperature decreases. The value of $R(T)$ at temperatures $T < T_{cf}$ depends on the current. This attests to a nonlinear current dependence of the differential resistance R_d of the heterojunction.

A family of curves of R_d versus the voltage V at various temperatures is shown in Fig. 3. It is evident that $R_d(0)$ increases as T decreases. This growth is reflected in an increase of the resistance $R(T)$ (Fig. 2). The nonlinearity observed in the IVC in the temperature range $72 \text{ K} < T < 84 \text{ K}$ is due to the destruction of the superconductivity of the YBCO film. The function $R_d(V)$ increases. This is due to the systematic destruction of superconductivity in sections of the YBCO electrode as the current I increases. We note that the

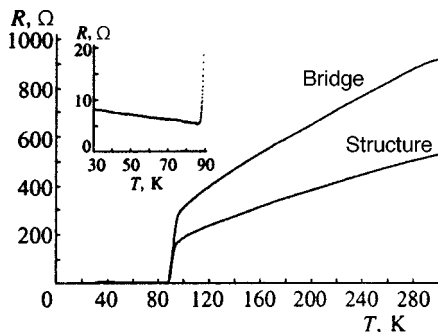


FIG. 2. Temperature dependence of the resistance of the heterostructure and of a 4 μm wide bridge arranged on the same substrate. Inset: $R(T)$, on an enlarged scale, of the heterojunction at temperatures $T < T_c$, where the resistance of the YBCO film is zero.

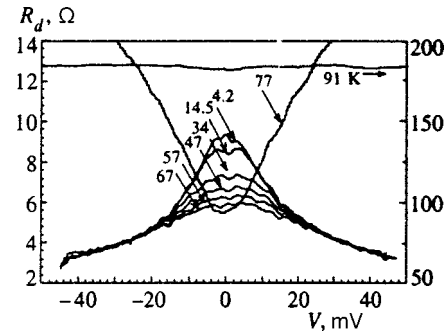


FIG. 3. Family of curves of the differential resistance of the heterojunction at various temperatures versus voltage. The scale along the resistance axis for $R_d(V)$ at $T=91$ K is shown on the right-hand side.

junction resistance at $T \approx T_{cf}$ is somewhat higher than the asymptotic resistance R_N , measured for $V > 20 \text{ mV}$ and $T \ll T_{cf}$.

The results of the measurements of the electrophysical parameters of several samples, prepared by the same method are presented in Table I. The resistance $R_N S$ of the boundary at $T=4.2$ K makes it possible to estimate the average (over the direction of the momentum of the quasiparticles) boundary transmittance, which we shall employ below,¹¹ as

$$\bar{D} = \frac{2\pi^2 \hbar^3}{e^2 p_F^2} \frac{1}{R_N S} = \frac{2\rho^{\text{YBCO}} l^{\text{YBCO}}}{3R_N S},$$

where p_F is the smallest value of the Fermi momentum for YBCO or Au.¹¹ The values of the transmittance of the boundaries of the fabricated structures for $\rho^{\text{YBCO}} l^{\text{YBCO}} \approx 3.2 \times 10^{-11} \Omega \cdot \text{cm}^2$ (Ref. 4) are also presented in Table I.

Test samples with bilayer heterostructures Au/YBCO, Nb/YBCO, and Au/Nb, fabricated using a technology with the same conditions as for the formation of the experimental Nb/Au/YBCO heterostructures, were also investigated. The resistances $R_N S$ of these boundaries measured at liquid-nitrogen temperature are $R_N S(\text{Au/YBCO}) \sim 10^{-8} \Omega \cdot \text{cm}^2$, $R_N S(\text{Au/Nb}) \sim 10^{-12} \Omega \cdot \text{cm}^2$, and $R_N S(\text{Nb/YBCO}) \sim 10^{-4} \Omega \cdot \text{cm}^2$. Here the series resistance of the YBCO film for $T_{cf} < 77 \text{ K}$ was taken into account. Comparing these quantities with the data presented in Table I, it is evident that the resistance of the Au/Nb boundary can be neglected, and the resistance of the Au/YBCO boundary, which increases when Nd is deposited on top of Au, probably, because of the interaction of Nb with YBCO, makes the main contribution to the resistance of the experimental heterojunctions. The resistance of a direct Nb/YBCO contact is very large. Most likely, the increase in the contact resistance is due to the displacement of oxygen out of the YBCO film into the Nb, which has good gettering characteristics, deposited on top. We note that the oxygen mobility in the a - b planes of YBCO is much higher than in the c direction.

Figure 4 shows the surface of a bilayer Au/YBCO heterostructure, measured with an atomic-force microscope. It is evident that its surface consists of Au granules separated by $\sim 1 \mu\text{m}$. The subsequently deposited Nb film covers the surface of the Au granules, where a good electric contact with the YBCO film is created, and forms a direct contact with

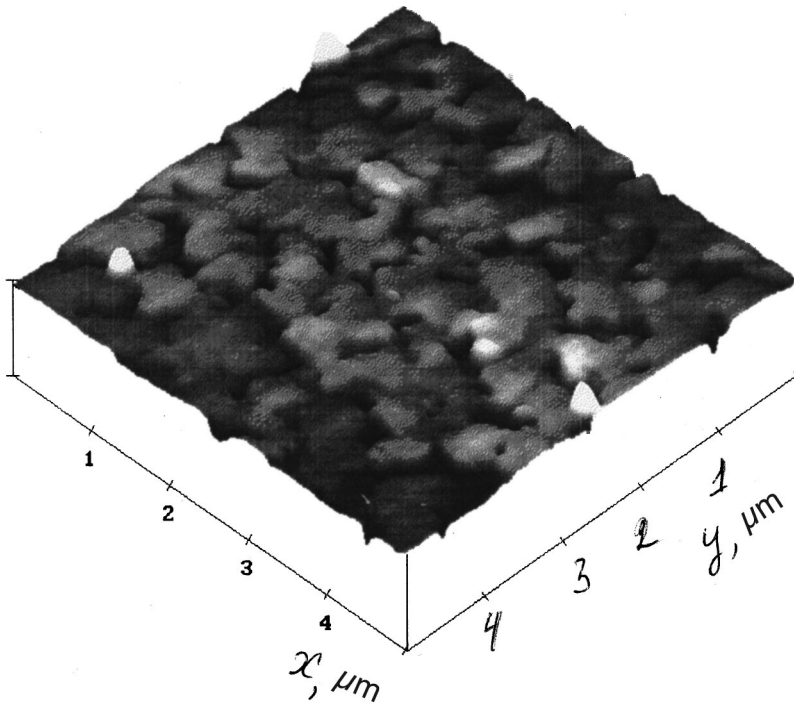


FIG. 4. Three-dimensional image of the surface of a bilayer heterostructure Au/YBCO. The image was obtained with an atomic-force microscope.

YBCO, where, as a result of a decrease in the amount of oxygen in the basal planes, the contact resistance is much higher. This could be the reason why the resistance of the trilayer heterostructure Nb/Au/YBCO is higher than that of a bilayer Au/YBCO heterostructure.

4. DISCUSSION OF THE EXPERIMENTAL RESULTS

The experimental trilayer heterostructure can be represented as Nb/Au/YBCO granules connected in parallel and sections of direct contact of Nb and YBCO via pores in the Au film. Since the characteristic resistance of the Nb/YBCO boundary is several orders of magnitude greater than $R_N S$ of the trilayer heterostructure Nb/Au/YBCO, and the surface area of the granules and pores, according to our estimates, differ severalfold (see Fig. 4), current flows mainly through the boundary of Nb/Au/YBCO granules. A trilayer Nb/Au/YBCO heterostructure can be described by the model shown in Fig. 5; a 100–150 nm superconducting YBCO electrode (S_d) with critical superconducting transition temperature $T_{cf}=87$ K; a 1–3 nm YBCO (S'_d) layer with an oxygen deficit and therefore disrupted superconducting properties; a 10–20 nm thick layer of normal metal (Au); a 100–150 nm thick superconducting Nb (S_s) electrode with $T_c=9.2$ K. A similar model has been proposed in Ref. 4 to estimate the electrophysical parameters of the system Pb/Au/YBCO.

First, we shall estimate the change in the superconducting order parameter in Nb as a result of the contact with Au. Since the measured value of the boundary resistance is quite small, it can be assumed that the superconducting Green's function, characterizing the amplitude of the interaction potential Φ of the superconducting carriers and its derivative with respect to the coordinate x are continuous at the boundary. Using the calculations of Refs. 12 and 13, we find that the superconducting order parameter Δ_1 of Nb at the Nb/Au

boundary is somewhat less than its equilibrium value Δ_{Nb} in the interior volume of the film and is $\Delta_1/e \approx 560 \mu V$. For estimates, the following values of the electrophysical parameters of Nb and Au were used at $T=4.2$ K: $\rho^{Nb} l^{Nb} = 4 \times 10^{-12} \Omega \cdot cm^2$, $\xi^{Nb} = 0.73 \times 10^{-6} cm$, $v_F^{Nb} = 3 \times 10^7 cm/s$, $T_{c0}^{Nb} = 9.2 K$ and $\rho^{Au} l^{Au} = 8 \times 10^{-12} \Omega \cdot cm^2$, $\xi^{Au} = 10^{-6} cm$, and $v_F^{Au} = 1.4 \times 10^8 cm/s$, where $v_F^{Nb,Au}$ is the Fermi velocity and $l^{Nb,Au}$ is the mean-free path length in Nb and Au, respectively.

Let us estimate the change in the order parameter at the YBCO/Au boundary. We assume that as a result of the interaction of YBCO and Nb, a superconducting surface layer S'_d of the order of 3 nm thick with critical temperature less than 4 K is formed.⁴ Assuming that the coherence length of S'_d differs negligibly from ξ_{c-YBCO} and is $\xi_{S'_d} = 5 \times 10^{-8} cm$ and that the resistivity increases by an order of magnitude⁴—from $\rho_{c-YBCO} = 10^{-4} \Omega \cdot cm^2$ to $\rho_{S'_d} = 1 \times 10^{-3} \Omega \cdot cm^2$, we obtain that at the Au/YBCO boundary

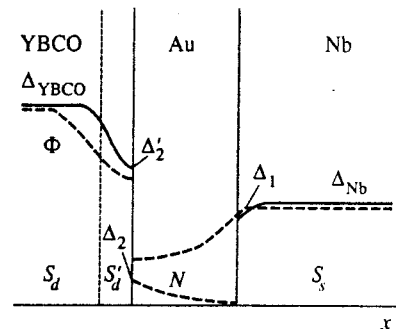


FIG. 5. Schematic diagram of the distribution of the order parameter (solid line) and the amplitude of the pair potential (dashed lines) in a direction perpendicular to the surface of an Nb/Au/YBCO heterostructure.

the order parameter decreases on the YBCO side decreases by a factor of approximately 100, $\Delta'_2/e \approx 140 \mu\text{V}$. A potential barrier with low transmittance, $\bar{D} \sim 10^{-6}$, is present at the Au/YBCO boundary. This barrier decreases Δ_2 by another factor of \bar{D} , $\Delta_2 = \Delta'_2 \bar{D}$. Here we used the theoretical estimates, which are strictly applicable for superconductors with *s*-type pairing. However, as the calculations of Refs. 10 and 14 show, the character of the change in the order parameter at the boundary of a *d* superconductor with a normal metal or insulator does not differ much from a junction with an *s* superconductor for orientations of the normal to the *d* superconductor along the principal crystallographic axes.

As a result, we can estimate the amplitude of the superconducting current through the entire structure by using the model of a superconductor—normal metal—superconductor (S'_dNS) junction, on the boundaries of whose weak section the values of the order parameters are known: $\Delta_2/e \approx 0.004 \mu\text{V}$ and $\Delta_1/e \approx 560 \mu\text{V}$. In what follows, we shall employ the theory developed for $S-N-S$ junctions. The thickness of the *N* layer is of the order of the coherence length, so that the change in the superconducting order parameter in the interlayer can be neglected. As a result, the product of the critical current I_c by R_N at low temperature is $I_c R_N \approx \sqrt{(\Delta_1 \Delta_2)/e} = 0.09 \mu\text{V}$. Taking account of the resistance of the heterojunctions ($R_N = 10 \Omega$), we obtain that the critical current of the structure $I_c \approx 0.009 \mu\text{A}$ is less than the fluctuation current $I_f = 1 \mu\text{A}$ of the measuring system and does not affect the experiment even if YBCO contains a mixture of *d* and *s* components of the superconducting order parameter and the number of *s* components is greater than the number of *d* components. For pure *d* pairing, the superconducting current for flow along the *c* direction in YBCO must be zero because of the type of symmetry of the superconducting order parameter. To estimate the critical current we assumed that the large width of the potential barrier (several coherence lengths) prevents direct tunneling of the superconducting current through the barrier. We note that we have considered quite strong suppression of the order parameter at the YBCO boundary because of degradation of the superconducting parameters of the HTSC film. However, even in the absence of suppression of the order parameter in the surface layer of YBCO, $\Delta_1/e = 14 \text{ mV}$, the critical current of the heterojunctions Nb/Au/YBCO will once again be comparable to the fluctuation current because of the decrease in the order parameter on the low-transmittance barrier.

The finite critical current, observed in a number of works,^{6–8} in Pb(Au,Ag)/YBCO heterostructures with a much larger value of $R_N S$ and large junction areas could be due to the fact that treatment of the YBCO electrode with a solution of bromine and alcohol, as was done in these works, opens up the basal planes of YBCO, the transmittance of whose boundaries with a normal metal or ordinary superconductors is three orders of magnitude higher than in the *c* direction ($R_{ab} S_{ab} \ll R_c S_c$). Ultimately, the superconducting current flows along the contacts to the basal plane of YBCO, and the normal resistance is determined by parallel connection of the resistances of the boundaries along the *c* and in the basal plane. In our case current flow is impeded in the direction of

the basal plane along the Nb/YBCO junctions, most likely because of substantial displacement of oxygen out of YBCO into Nb.

It is important that lead can react with Au, forming a superconducting alloy. Then, the Pb/Au/YBCO structure contains a superconductor instead of a layer of normal metal. This is confirmed by the appearance of gap features of lead in the IVCs^{6–8} at sufficiently low temperatures ($T = 1.2 \text{ K}$).

A new explanation of the experimental data on the flow of a superconducting current through low-temperature superconductor—HTSC junctions was proposed recently. It has been shown theoretically¹⁵ that a strong spin-orbit interaction, which is observed in Pb/Ag structures, intensifies superconducting current flow through a barrier. Replacement of Pb by an Al- or Nb-type superconductor decreases the spin-orbit interaction, and the superconducting current decreases as a result.

Let us discuss the dependences $R_d(V)$ for heterojunctions as a function of temperature in the range 4.2–100 K (Fig. 3). For $T \ll T_c$ the IVC as a whole corresponds to heterojunctions of the type superconductor—insulator—normal metal ($S-I-N$): There is a location where R_d increases at low voltages. However, the feature on $R_d(V)$ that is due to the gap in YBCO is not observed in the experiment. This corresponds to a junction with a superconductor with gapless superconductivity, including with *d*-type superconductivity.^{14,16,17} According to the calculations performed in Ref. 14, the feature at $eV \approx \Delta$ in the density of states of a *d* superconductor gives a logarithmic dependence $R_d \propto \ln(T)$, $\ln(|eV| - |\Delta|)$, subjected to strong temperature broadening just as for a gapless *s* superconductor. We note that for *s* superconductors with a gap a power-law divergence is observed $R_d \propto T^{-1/2} ((eV)^2 - \Delta^2)^{-1/2}$. The features in the form of changes in $R_d(V)$ at voltages $V < 2 \text{ mV}$ due to the niobium gap have virtually no effect in our experiment, and we did not study them in detail.

For *s*-type symmetry of the order parameter in a superconductor at low temperatures, $kT \ll \Delta$, the number of excited quasiparticles decreases exponentially with temperature. Therefore the resistance increases proportionally $R_d(0) \propto (-\Delta/T)$.¹⁷ In a superconductor with *d*-type pairing, the presence of nodes with a zero order parameter makes it possible to excite a quasiparticle even at very low temperature, $T \ll \Delta$. As a result, $R_d(0)$ grows more slowly as temperature decreases.¹⁴ As one can see in the inset in Fig. 2, nearly linear growth of $R_d(0)$ with decreasing T is observed in the experiment. The dependence $R_d(V)$ is quadratic as $V \rightarrow 0$, which agrees qualitatively with calculations for a *d* superconductor.¹⁴

One of the most surprising features of superconductors with *d*-type pairing is the appearance of two types of bound states, which, as a rule, are not observed in *s*-superconductors.¹⁷ Surface states with low energies at the boundary of the *d* superconductor with an insulator are due to the change in sign of the order parameter at the Fermi surface for quasiparticles reflected from the boundary.^{16,17} The superconducting parameter for a *d*-type superconducting wave function changes sign with a 90° circuit around the *c* axis. Since the direction of the momentum of a quasiparticle

changes on mirror reflection from a boundary, bound states arise at zero energies because of Andreev reflection. This leads to the appearance of a dip in $R_d(V)$ at small V , as is observed experimentally for a transport current in the [110] direction in a YBCO film (see Refs. 6–8, 18, and 19). In our case, the contribution of such quasiparticles is small because the normal to the boundary is oriented along one of the principal crystallographic directions in YBCO. For mirror-reflected quasiparticles, there is no Andreev reflection because the phases of the order parameter are the same for incident and reflected quasiparticles.

An additional mechanism was recently predicted theoretically for the appearance of bound states due to the suppression of the order parameter of a d -superconductor for orientations of the normal with respect to the boundary different from the principal crystallographic axes or for diffuse reflection at a boundary with an insulator.¹⁷ These states are observed at energies different from zero, and estimates in Ref. 17 show that they are more stable with respect to the quality of the boundary. The appearance of bound states should be observed in the dependences $R_d(V)$ as a decrease of R_d for eV_r of the order of the gap in the d -superconductor, and in addition the ratio eV_r/Δ depends on the angle between the normal and the crystallographic axes of the d -superconductor. The condition for the existence of bound states with nonzero energy is suppression of the order parameter near the boundary. This occurs in our experiment because of the degradation of the superconducting properties of the surface. Indeed, in all samples we observe features at $V_r=15$ mV, where V_r is virtually temperature-independent.

5. CONCLUSIONS

In the present work, heterojunctions with dimensions of several microns, obtained by successive deposition of YBCO, Au, and Nb, with transport current flowing in YBCO along the c axis were fabricated and studied experimentally. The transmittances of the heterostructures, as estimated from the resistance of the junctions, are two orders of magnitude greater than the existing experimental data, and the areas of the heterojunctions are much smaller. The IVCs of the heterojunctions with resistances differing from one another by a factor of 4 were investigated. Estimates based on the proximity effect showed that the absence of a critical current in heterojunctions is probably due to a decrease in the amplitude of the potential of the superconducting carriers at the Au/YBCO boundary. The curves of the differential resistance of the heterojunctions versus the voltage are similar to

the case of $S-I-N$ junctions with a gapless superconductor, specifically, the absence of a YBCO gap feature could also correspond to d -type superconductivity, specifically, to the presence of nodes of the order parameter as the direction of the momentum of the quasiparticles changes by 45° . The dependence of $R_d(0)$ on T also corresponds to a d -type superconductor.

We thank Yu. S. Barash, D. A. Golubev, A. V. Zaitsev, Z. G. Ivanov, and M. Yu. Kupriyanov for a helpful discussion of the experimental results, and D. Ertz, P. B. Mozhaev, and T. Henning for assisting in the experiment.

This work was supported in part by the program ‘‘Current Problems of Condensed-State Physics’’ (subsection ‘‘Superconductivity’’), the Russian Fund for Fundamental Research, and the INTAS program of the European Union.

*E-mail: gena@lab235.cplire.ru

- ¹D. A. Wollman, D. J. Van Harlingen, W. C. Lee *et al.*, Phys. Rev. Lett. **71**, 2134 (1993).
- ²C. C. Tsuei, J. R. Kirtley, C. C. Chi *et al.*, Phys. Rev. Lett. **73**, 593 (1994).
- ³H. Akoh, C. Camerlingo, and S. Takada, Appl. Phys. Lett. **56**, 1487 (1990).
- ⁴J. Yoshida, T. Hashimoto, S. Inoue *et al.*, Jpn. J. Appl. Phys., Part 1 **31**, 1771 (1992).
- ⁵J. Lesueur, L. H. Greene, W. L. Feldmann *et al.*, Physica C **191**, 325 (1992).
- ⁶A. G. Sun, A. Truscott, A. S. Katz *et al.*, Phys. Rev. B **54**, 6734 (1996).
- ⁷A. S. Katz, A. G. Sun, R. C. Dynes *et al.*, Appl. Phys. Lett. **66**, 105 (1995).
- ⁸J. Lesueur, M. Aprili, A. Goulon *et al.*, Phys. Rev. B **55**, 3398 (1997).
- ⁹J. R. Kirtley, K. A. Moler, and D. J. Scarlapino, E-print archive cond-mat/9703067 (1997).
- ¹⁰L. J. Buchholtz, M. Palumbo, D. Rainer, and J. A. Sauls, J. Low Temp. Phys. **101**, 1099 (1995).
- ¹¹A. V. Zaitsev, Zh. Eksp. Teor. Fiz. **86**, 1742 (1984) [Sov. Phys. JETP **59**, 1015 (1984)].
- ¹²M. Yu. Kupriyanov and K. K. Likharev, IEEE Trans. Magn. **27**, 2400 (1991).
- ¹³G. Deutscher, Physica C **185–189**, 216 (1991).
- ¹⁴Yu. S. Barash, A. V. Galaktionov, and A. D. Zaikin, Phys. Rev. B **52**, 665 (1995).
- ¹⁵G. S. Lee, Physica C **292**, 171 (1997).
- ¹⁶Y. Tanaka and S. Kashiwaya, Phys. Rev. B **53**, 11957 (1996).
- ¹⁷Yu. S. Barash, A. A. Svidzinsky, and H. Burkhardt, Phys. Rev. B **55**, 15282 (1997).
- ¹⁸F. V. Komissinskiĭ, G. A. Ovsyannikov, N. A. Tulina, and V. V. Ryazanov, in *Abstracts of Reports at the 31st Conference on Low-Temperature Physics (LT-31)*, Moscow, 1998, p. 236.
- ¹⁹P. V. Komissinskiĭ, G. A. Ovsyannikov, N. A. Tulina, and V. V. Ryazanov, E-print archive cond-mat/9903065 (1999).

Translated by M. E. Alferieff